Inorganic Chemistry

Article

pubs.acs.org/IC

Halide-Bridged Binuclear HX-Splitting Catalysts

David C. Powers, Seung Jun Hwang, Shao-Liang Zheng, and Daniel G. Nocera*

Department of Chemistry and Chemical Biology, Harvard University, 12 Oxford Street, Cambridge, Massachusetts 02138, United States

Supporting Information

ABSTRACT: Two-electron mixed-valence compounds promote the rearrangement of the two-electron bond photochemically. Such complexes are especially effective at managing the activation of hydrohalic acids (HX). Closed HX-splitting cycles require proton reduction to H_2 and halide oxidation to X_2 to be both accomplished, the latter of which is thermodynamically and kinetically demanding. Phosphazane-bridged Rh_2 catalysts have been especially effective at activating HX via photogenerated ligand-bridged intermediates; such intermediates are analogues of the classical ligand-bridged intermediates proposed in binuclear elimination reactions. Herein, a new family of phosphazane-bridged Rh_2 photocatalysts has been developed where the halide-bridged geometry is designed into the ground state. The targeted geometries were accessed by replacing previously used alkyl isocyanides with aryl isocyanide ligands, which provided access to families of Rh_2L_1 complexes. H_2 evolution with Rh_2 catalysts typically proceeds via two-electron photoreduction, protonation to afford Rh hydrides, and photochemical H_2 evolution. Herein, we have directly observed each of these steps in stoichiometric reactions. Reactivity differences between Rh_2 chloride and bromide complexes have been delineated. H_2 evolution from both HCl and HBr proceeds with a halide-bridged Rh_2 hydride photoresting state. The H_2-evolution efficiency of the new family of halide-bridged catalysts is compared to a related catalyst in which ligand-bridged geometries are not stabilized in the molecular ground state, and the new complexes are found to more efficiently facilitate H_2 evolution.

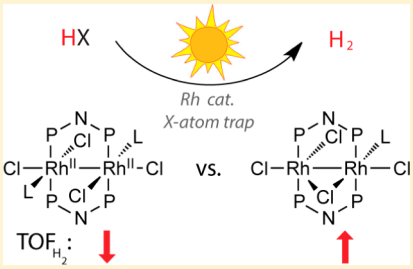

INTRODUCTION

The multielectron/multiproton transformations involved in the splitting of water or hydrohalic acids (HX) to generate energy-rich solar fuels (H_2 and O_2 or X_2) implicitly involve substantial thermodynamic and kinetic barriers.[1−5] Photochemical splitting of HX requires the management of two electrons and two protons.[6−9] We have developed the design principle of two-electron mixed-valency, $M^n\cdots M^{n+2}$, to promote multielectron/multiproton transformations. These endeavors have been guided by the hypothesis that ground-state two-electron mixed valency will give rise to molecular excited states capable of mediating multielectron photoreactions without participating in the parasitic single-electron transformations that are frequently encountered in inorganic photochemistry.[10,11] Specifically, redox cooperativity may be established between the individual metal centers of a mixed-valence core such that two-electron oxidations may be promoted at an M^{n+2} center and two-electron reductions may be promoted at an M^n center.[12−14] Hydrogen addition and elimination from $M^n\cdots M^{n+2}$ cores is driven through a hydrogen-bridged intermediate (eq 1).[15] In this manner, the two-electron mixed valency of the core may be preserved, and hence, reorganization energy is minimized.

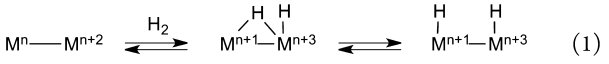

(1)

Dirhodium[II,II] complex **1** has recently been disclosed as a competent catalyst for H_2 evolution from HCl in the presence of halogen traps.[16] Examination of the time-resolved photochemistry of complex **1** revealed the presence of a discrete photointermediate, which was proposed to be chloride-bridged Rh_2 complex **2**. The chloride-bridged intermediate underpins the photocycle shown in Figure 1, which comprises three distinct photochemical steps for net HX splitting. From photoresting state **1**, photochemical extrusion of an isocyanide ligand generates chloride-bridged intermediate **2**. Subsequent halogen photoelimination from **2** affords Rh_2[0,II] complex **3**, which undergoes thermal reaction with HCl to afford hydrido chloride **4**. Finally, photochemical reaction of **4** with exogenous HCl evolves H_2 and regenerates Rh_2 complex **1**.

The ligand-bridged geometry of the two-electron core (i.e., **2**) is reminiscent of hydride-bridged intermediates of the binuclear elimination mechanism described by Norton for binuclear elimination reaction of Os alkyl hydrides.[17−19] In effect, the two-electron mixed-valence core permits such an intermediate to be established intramolecularly, thus bypassing the need for a bimolecular reaction to achieve elimination. The potential relevance of such intermediates to promoting the elimination reactions of more energy intensive processes such as HX splitting has not been investigated.

Photointermediate **2** is short-lived (τ = 13 μs), which is typical of unsaturated structures generated by ligand photoextrusion chemistry.[20] We hypothesized that, if a Rh_2 structure supported by a single monodentate L-type ligand (Rh_2L_1)

Received: May 15, 2014
Published: August 19, 2014

   dx.doi.org/10.1021/ic501136m | Inorg. Chem. 2014, 53, 9122−9128

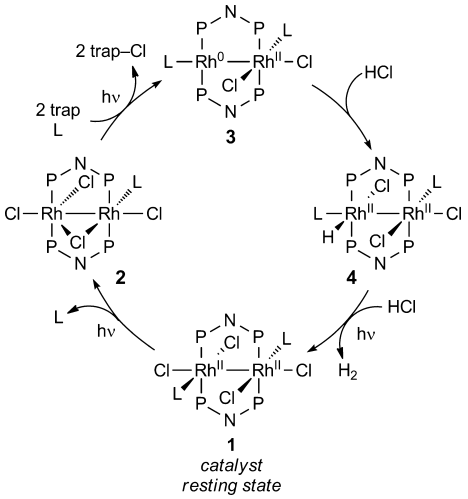

Figure 1. HX splitting catalyzed by **1** proceeds via photoinduced ligand dissociation from catalyst resting state **1**, two-electron photoreduction of chloride-bridged complex **2**, protonation of Rh_2[0,II] complex **3**, and photoinduced H_2 evolution from Rh_2 hydride **4**. Three sequential photochemical steps are involved in the overall cycle; L = 1-adamantylisocyanide, P–N–P = bis(trifluoroethoxy)phosphino)methylamine (tfepma).

could be stabilized, the need for photochemically driven ligand dissociation (i.e., conversion of **1** to **2**, Figure 1) would be obviated. Stabilization of the chloride-bridged intermediate would provide a structure poised to directly engage in multielectron photoelimination chemistry. Accordingly, if a Rh_2L_1 structure were employed as a photocatalyst for HX splitting, the catalysis cycle depicted in Figure 2, which relies on

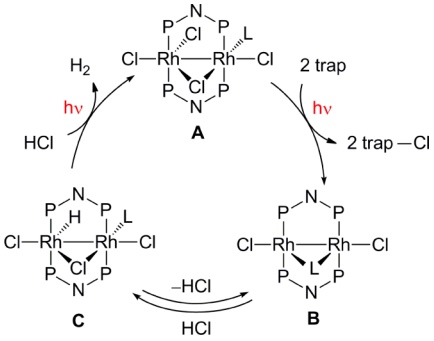

Figure 2. A photocycle involving a halide-bridged resting state for HX, which has two photochemical steps instead of the three involved in catalysis with complex **1**.

two, not three, photochemical steps, could be accomplished. Herein, we report new HX-splitting photocatalysts that have been designed on the premise that halide-bridged structures may facilitate X_2 elimination photochemistry. HX-splitting photocatalysis is observed to proceed with a halide-bridged binuclear Rh hydride photoresting state, which represents the first example of a reaction in which halide oxidation is not the turnover-limiting step of HX-splitting photocatalysis. Furthermore, H_2-evolving catalysis with Rh_2L_1 catalysts is observed to be more efficient than HX splitting catalyzed by Rh_2L_2 analogues.

EXPERIMENTAL SECTION

General Considerations. All reactions were carried out in a N_2-filled glovebox. Anhydrous solvents were obtained by filtration through drying columns.[21] $[Rh(cod)Cl]_2$ and HCl·dioxane were obtained from Strem Chemicals and Sigma-Aldrich, respectively, and were used without purification. A saturated HBr solution in CH_2Cl_2 was prepared by bubbling $HBr_{(g)}$ through CH_2Cl_2 at 293 K; the concentration was assumed to be ~0.5 M HBr.[22] Ligand tfepma,[23] complexes **1**, **4**,[14] **5**, **6**, **8**, and **9**,[16] and $[Rh(cod)Br]_2$[24] were prepared as previously described. Experimental details of X-ray crystallography are in the Supporting Information. Crystal data and refinement statistics are summarized in Table 1, and thermal ellipsoid plots are collected in Figures 3 and 4. X-ray data for **6** is available as CCDC 925037.

Physical Methods. NMR spectra were recorded at the Harvard University Department of Chemistry and Chemical Biology NMR facility on a Varian Unity/Inova 600 spectrometer operating at 600 MHz for ^{1}H acquisitions, a Varian Unity/Inova 500 spectrometer operating at 500 MHz for ^{1}H acquisitions, or a Varian Mercury 400 spectrometer operating at 400 HMz for ^{1}H acquisitions. NMR chemical shifts are reported in parts per million (ppm) with the residual solvent resonance as internal standard. UV–vis spectra were recorded at 293 K in quartz cuvettes on a Spectral Instruments 400 series diode array, and blanks were performed against the appropriate solvent. IR spectra were recorded on a PerkinElmer Spectrum 400 FT-IR/FT-FIR spectrometer outfitted with a Pike Technologies GladiATR attenuated total reflectance accessory with a monolithic diamond stage and pressure clamp. IR measurements were carried out on powdered samples, except for hydride complexes, in which case, samples were suspended in Nujol. Steady-state photochemical reactions were performed using a 1000 W high-pressure Hg/Xe arc lamp (Oriel), and the beam was passed through a water-jacketed filter holder containing the appropriate long-pass filter, an iris, and a collimating lens.

Rh_2(tfepma)$_2$(p-F-C_6H_4NC)(μ-Cl)Cl_2H (7). To a solution of Rh_2(tfepma)$_2$(μ-p-F-C_6H_4NC)Cl_2 (**5**) (31.0 mg, 2.28×10^{-5} mol, 1.00 equiv) in THF (0.5 mL) at 23 °C was added HCl·dioxane (4.0 M, 0.10 mL, 3.4×10^{-4} mol, 15 equiv) in one portion. The color of the reaction mixture turned from orange to dark red. Solution characterization (^{1}H, ^{19}F, and ^{31}P{^{1}H} NMR and UV–vis) was carried out using the reaction solution without further purification because removal of solvent afforded a mixture of Rh_2 hydride **7** and Rh_2[I,I] complex **5**. Based on integration of the ^{1}H NMR spectrum against hexamethylbenzene (internal standard), the yield of **7** was 95%. ^{1}H NMR (400 MHz, CD_2Cl_2) δ (ppm): 7.26 (dd, J = 9.2 Hz, J = 4.9 Hz, 2H), 7.18 (dd, J = 7.9 Hz, J = 7.9 Hz, 2H), 4.93–4.72 (m, 8H), 4.71–4.63 (m, 6H), 4.40–4.38 (m, 2H), 3.01 (pseudoquintet, J = 3.9 Hz, 6H), −19.40 (dt, J = 25.0 Hz, J = 10.0 Hz, 1H). ^{31}P{^{1}H} NMR (121.5 MHz, CD_2Cl_2) δ (ppm): 127.4–125.1 (m, 2P), 111.2–109.1 (m, 2P). ^{19}F NMR (275 MHz, CD_2Cl_2) δ (ppm): −81.9, −82.3 (m, 24F), −114.1 (br s, 1F). IR: ν_{CN} = 2171 cm^{-1}. Crystals suitable for single-crystal diffraction analysis were obtained from a THF solution layered with pentane at −30 °C. Satisfactory combustion analysis could not be obtained because **7** was not stable to evacuation of solvent.

Rh_2(tfepma)$_2$(p-MeO-C_6H_4NC)(μ-Cl)Cl_2H (10). To a solution of Rh_2(tfepma)$_2$(μ-p-MeO-C_6H_4NC)Cl_2 (**8**) (38.8 mg, 2.23×10^{-5} mol, 1.00 equiv) in THF (0.5 mL) at 23 °C was added HCl·dioxane (4.0 M, 0.10 mL, 3.4×10^{-4} mol, 15 equiv) in one portion. The color of the reaction mixture turned from orange to dark red. Solution characterization (^{1}H, ^{19}F, and ^{31}P{^{1}H} NMR and UV–vis) was carried out using the reaction solution without further purification because removal of solvent afforded a mixture of Rh_2 hydride **10** and Rh_2[I,I] complex **8**. Based on integration of the ^{1}H NMR spectrum against hexamethylbenzene (internal standard), the yield of **10** was 90%. ^{1}H NMR (400 MHz, CD_2Cl_2) δ (ppm): 7.18 (d, J = 8.8 Hz, 2H), 6.93 (d, J = 8.8 Hz, 2H), 4.92–4.87 (m, 2H), 4.81–4.70 (m, 6H), 4.70–4.56 (m, 6H), 4.40–4.32 (m, 2H), 3.85 (s, 3H), 2.98 (pseudoquintet, J = 3.3 Hz, 6H), −19.44 (td, J = 35.6 Hz, J = 10.9 Hz, 1H). ^{31}P{^{1}H} NMR (121.5 MHz, THF-d_8) δ (ppm): 134.5–132.1 (m, 2P), 118.3–116.2 (m, 2P). IR: ν_{CN} = 2170 cm^{-1}. Crystals suitable

dx.doi.org/10.1021/ic501136m | Inorg. Chem. 2014, 53, 9122–9128

Table 1. Crystal Data and Structure Refinement

	7	10·$PhCH_3$	11	12	13·$PhCH_3$
formula	$C_{25}H_{27}Cl_3F_{25}N_3O_8P_4Rh_2$	$C_{33}H_{38}Cl_3F_{24}N_3O_9P_4Rh_2$	$C_{25}H_{26}Br_2F_{25}N_3O_8P_4Rh_2$	$C_{25}H_{24}Br_4F_{25}N_3O_8P_4Rh_2$	$C_{32}H_{33}Br_3F_{25}N_3O_8P_4Rh_2$
CCDC No.	986358	986359	986360	986361	986362
fw, g/mol	1408.55	1512.72	1461.01	1618.81	1634.06
temp, K	100(2)	100(2)	100(2)	100(2)	15(2)
cryst system	triclinic	triclinic	triclinic	monoclinic	triclinic
space group	$P\bar{1}$	$P\bar{1}$	$P1$	Cm	$P\bar{1}$
color	orange	orange	orange	orange	orange
a, Å	11.352 (1)	11.3961 (4)	10.300 (1)	14.074 (2)	11.3409 (8)
b, Å	15.620 (2)	15.6785 (6)	10.320 (1)	21.280 (3)	15.516 (1)
c, Å	16.158 (2)	17.1337 (6)	12.224 (1)	9.609 (2)	16.365 (1)
α, deg	73.874 (3)	69.7710 (6)	68.119 (2)	90	72.801 (1)
β, deg	88.470 (3)	86.0740 (6)	73.780 (2)	124.859 (2)	88.991 (1)
γ, deg	69.556 (2)	68.9300 (5)	72.190 (2)	90	70.77 (1)
V, A^3	2571.1 (5)	2675.0 (2)	1127.6 (2)	2361.3 (6)	2587.4 (3)
Z	2	4	1	2	2
$R1^a$	0.097	0.030	0.061	0.057	0.043
$wR2^b$	0.230	0.069	0.109	0.091	0.136
GOF $(F^2)^c$	1.09	1.05	1.01	1.00	1.09
R_{int}	0.140	0.039	0.047	0.106	0.049

$^a R1 = \sum||F_o| - |F_c||/\sum|F_o|$. $^b wR2 = (\sum(w(F_o^2 - F_c^2)^2)/\sum(w(F_o^2)^2))^{1/2}$. $^c GOF = (\sum w(F_o^2 - F_c^2)^2/(n-p))^{1/2}$, where n is the number of data and p is the number of parameters refined.

for single-crystal diffraction analysis were obtained from a THF solution layered with $PhCH_3$ at −30 °C. Satisfactory combustion analysis could not be obtained because **10** was not stable to evacuation of solvent.

Rh_2(tfepma)$_2$(μ-*p*-F-C_6H_4NC)Br_2 (11). To a solution of [Rh(cod)Br]$_2$ (114 mg, 1.96×10^{-4} mol, 1.00 equiv) in THF (4.0 mL) tfepma (191 mg, 3.93×10^{-4} mol, 2.00 equiv) and *p*-fluorophenylisocyanide (47.6 mg, 3.93×10^{-4} mol, 2.00 equiv) were added sequentially. The dark red reaction solution was stirred at 23 °C for 4 h. Solvent was removed in vacuo, and the residue was taken up in THF (1 mL) and hexanes (10 mL). The supernatant was removed, and the solid residue was dried in vacuo to afford 203 mg of the title complex (70.8% yield) as an orange solid. ^{1}H NMR (600 MHz, CD_2Cl_2) δ (ppm): 7.29 (dd, J = 8.9 Hz, J = 4.8 Hz, 2H), 7.03 (dd, J = 8.7 Hz, J = 8.7 Hz, 2H), 4.68−4.56 (m, 16H), 2.79 (pseudoquintet, J = 3.5 Hz, 6H). ^{31}P{^{1}H} NMR (121.5 MHz, CD_2Cl_2) δ (ppm): 129.0 (m, 4P). ^{19}F NMR (275 MHz, CD_2Cl_2) δ (ppm): −75.3, −75.2 (m, 24F), −115.3 (br s, 1F). IR: ν_{CN} = 1735 cm^{-1}. Crystals suitable for single-crystal diffraction analysis were obtained from a CH_2Cl_2 solution layered with $PhCH_3$ at −30 °C.

Rh_2(tfepma)$_2$(*p*-F-C_6H_4NC)(μ-Br)Br_3 (12). To a solution of Rh_2(tfepma)$_2$(μ-*p*-F-C_6H_4NC)Br_2 (**11**) (15.8 mg, 1.08×10^{-5} mol, 1.00 equiv) in CH_2Cl_2 (1.5 mL) at 23 °C was added Br_2 (2.2 mg, 0.70 μL, 1.4×10^{-5} mol, 1.3 equiv) as a solution in CH_2Cl_2 (0.5 mL). The color of the reaction solution turned from orange to red. After stirring for 30 min at 23 °C, solvent was removed in vacuo to afford 17.4 mg of the title complex (99.3% yield) as a dark orange solid. ^{1}H NMR (400 MHz, CD_2Cl_2) δ (ppm): 7.50 (dd, J = 4.7 Hz, J = 1.9 Hz, 2H), 7.48 (dd, J = 4.6 Hz, J = 4.6 Hz, 2H), 4.95−4.86 (m, 4H), 4.82−4.68 (m, 8H), 4.55−4.48 (m, 2H), 4.44−4.36 (m, 2H), 3.01 (pseudoquintet, J = 3.5 Hz, 6H). ^{31}P{^{1}H} NMR (121.5 MHz, CD_2Cl_2) δ (ppm): 110.9 (m, 4P). ^{19}F NMR (275 MHz, CD_2Cl_2) δ (ppm): −74.8 (t, J = 9.2 Hz, 6F), −75.1 (m, 12F), −75.2 (t, J = 9.2 Hz, 6F), −106.4 (br s, 1F). IR: ν_{CN} = 2190 cm^{-1}. Crystals suitable for single-crystal diffraction analysis were obtained from a CH_2Cl_2 solution layered with $PhCH_3$ at −30 °C.

Rh_2(tfepma)$_2$(*p*-F-C_6H_4NC)(μ-Br)Br_2H (13). To a solution of Rh_2(tfepma)$_2$(μ-*p*-F-C_6H_4NC)Br_2 (**11**) (32.7 mg, 2.23×10^{-5} mol, 1.00 equiv) in CH_2Cl_2 at 23 °C was added sat. HBr in CH_2Cl_2 (0.5 M, 0.20 mL, 8.6×10^{-5} mol, 4.0 equiv) in one portion. The color of the reaction mixture turned from orange to dark red. Solution characterization (^{1}H, ^{19}F, and ^{31}P{^{1}H} NMR and UV−vis) was carried out using the reaction solution without further purification because removal of solvent afforded a mixture of Rh_2 hydride **13** and Rh_2[I,I] complex **11**. Based on integration of the ^{1}H NMR spectrum against hexamethylbenzene (added as internal standard), the yield of **13** was 95%. ^{1}H NMR (600 MHz, CD_2Cl_2) δ (ppm): 7.24 (dd, J = 9.3 Hz, J = 5.0 Hz, 2H), 7.16 (dd, J = 7.9 Hz, J = 7.9 Hz, 2H), 4.88−4.72 (m, 8H), 4.68−4.59 (m, 6H), 4.40−4.34 (m, 2H), 2.97 (pseudoquintet, J = 3.8 Hz, 6H), −18.30 (dt, J = 21.6 Hz, J = 10.1 Hz, 1H). ^{31}P{^{1}H} NMR (121.5 MHz, CD_2Cl_2) δ (ppm): 117.5 (m, 2P), 99.9 (m, 2P). ^{19}F NMR (275 MHz, CD_2Cl_2) δ (ppm): −74.5 (m, 24F), −107.0 (br s, 1F). IR: ν_{CN} = 2171 cm^{-1}. Crystals suitable for single-crystal diffraction analysis were obtained from a CH_2Cl_2 solution layered with $PhCH_3$. Satisfactory combustion analysis could not be obtained because **13** was not stable to evacuation of solvent.

Photochemistry. Compounds **1**, **6**, **9**, and **12** were photolyzed with the broadband excitation light delivered from a 1000 W Hg/Xe arc lamp; samples were photolyzed in a constant temperature water bath. THF solutions of the complexes were photolyzed in 1 cm quartz cuvettes. Reaction samples were periodically removed from the light source, and UV−vis spectra were recorded. Photolysis spectra (λ_{exc} > 295 nm) of THF solutions are shown in Figures S23 (**6**) and S25 (**9**) (Supporting Information) and Figure 5a (**12**). Photolysis spectra (λ_{exc} > 295 nm) of THF solutions in the presence of HCl are shown in Figure 6b (**6**) and Figure S26 (**9**) (Supporting Information) and a photolysis spectra of a THF solution of **12** in the presence of HBr is shown in Figure S28 (Supporting Information). Photocatalysis experiments were carried out with 1.0 mM loading of Rh_2 complexes in 0.1 M HX (X = Cl or Br) solutions in THF; at the employed catalyst concentration, all incident light from the Hg arc lamp was absorbed (abs. ≥ 1.5 for 300 < λ < 500 nm). Evolved hydrogen was quantified by gas chromatography and Toepler pump combustion analysis.

RESULTS AND DISCUSSION

Synthesis, Characterization and Photochemistry. Each of the proposed steps in the targeted photocycle drawn in Figure 2, (i) photoreduction of a chloride-bridged binuclear complex to a ligand-bridged Rh_2[I,I] complex, (ii) protonation to afford a chloride-bridged Rh_2 hydride, and (iii) photoevolution of H_2 by photolysis of the Rh_2 hydrides in the presence of acid, has been independently examined using isolated Rh_2 complexes.

dx.doi.org/10.1021/ic501136m | Inorg. Chem. 2014, 53, 9122−9128

The suite of Rh_2L_1 complexes needed to interrogate the photocycle of Figure 2 was accessed by the sequential treatment of [RhCl(cod)]$_2$ with phosphazane tfepma and substituted aryl isocyanides, followed by oxidation with $PhICl_2$; use of 4-F-C_6H_4NC provided ready access to chloride-bridged Rh_2 tetrachloride complex **6** (Figure 3). Photolysis of THF solutions of **6** featuring a terminal isocyanide ligand (ν_{CN} = 2181 cm^{-1}) affords Rh_2[I,I] complex **5** with a bridging isocyanide ligand (ν_{CN} = 1736 cm^{-1}) in 97% yield, which establishes the viability of two-electron photoreduction of (μ-Cl)Rh_2 complexes (step **A** → **B**, Figure 2). Photoreduction requires the presence of potential halogen-radical traps (i.e., THF); photolysis of a PhH solution of **7** does not result in photoreduction. Cl-atom trapping by THF via H-atom abstraction (HAA) would generate HCl and a furanyl radical, which could participate in a variety of subsequent transformations.[25,26] The furanyl-radical derived products under these conditions have not been identified.

Treatment of photogenerated Rh_2[I,I] complex **5** with HCl afforded a new complex, which we assign to be Rh_2 hydride complex **7** (98% yield). The spectral details supporting this assignment are outlined below. The ^{1}H NMR spectrum contained signals attributable to one 4-fluorophenylisocyanide ligand, two tfepma ligands, and an additional resonance at −19.40 ppm (dt, $^1J_{Rh-H}$ = 25.0 Hz, $^2J_{P-H}$ = 10.0 Hz), which integrated for a single proton (Figure 3b). The ^{31}P{^{1}H} NMR spectrum displayed two multiplets centered at 110 and 126 ppm; a ^{1}H−^{31}P HMQC experiment established coupling of the ^{31}P resonance at 126 ppm to the ^{1}H resonance at −19.40 ppm (Figure S3, Supporting Information). The IR spectrum displayed a ν_{CN} = 2171 cm^{-1} (Figure S17, Supporting Information), consistent with a terminally bound isocyanide ligand.[27−29] Removal of the reaction solvent and redissolution of the residue afforded a mixture of Rh_2 hydride **7** and Rh_2[I,I] complex **5**. Single crystals of Rh_2 hydride **7** were obtained by layering the reaction mixture with $PhCH_3$, and X-ray diffraction analysis established the molecular structure of **7** to be the chloride-bridged Rh_2 complex shown in Figure 3a. The hydride ligand was not located in the difference map, but its presence was inferred by examination of the bond lengths between the bridging chloride ligand and each of the Rh centers; Rh(2)−Cl(1) (trans to isocyanide ligand): 2.467(3) Å, while Rh(1)−Cl(1) (trans to hydride ligand): 2.530(3) Å. The asymmetry in the Rh−Cl distances to the bridging ligand is consistent with the strong trans influence of the hydride ligand as compared to the isocyanide ligand.[30] For comparison, Rh−Cl bond distances for chloride-bridged complex **6** are 2.421(2) and 2.404(2) Å, respectively. The oxidative addition of HCl to **5** to generate Rh_2 hydride **7** confirms the viability of the transformation of **B** to **C** in Figure 2. Finally, photolysis of **7** in the presence of HCl leads to the evolution of H_2 without consumption of **7** (vide infra, photocatalysis section). Consistent with the requirement for photochemical, not thermal, H_2 evolution, treatment of Rh_2 hydride **7** with excess HCl does not lead to the thermal evolution of H_2. The failure to produce H_2 thermally upon treatment of **7** with HCl is consistent with a previous report of diminished hydricity of related Rh_2 hydride complexes.[31]

Rh_2L_1 complex **9**, supported by a 4-$MeOC_6H_4NC$ ligand, participates in a similar manifold of photochemical reactions as does Rh_2L_1 complex **6** (Figure 3a). Complex **9** undergoes clean photoreduction to Rh[I,I] complex **8**, which can be converted to Rh_2 hydride **10** upon treatment with HCl. The spectral features observed for hydride **10** (^{1}H and ^{31}P{^{1}H} NMR, IR)

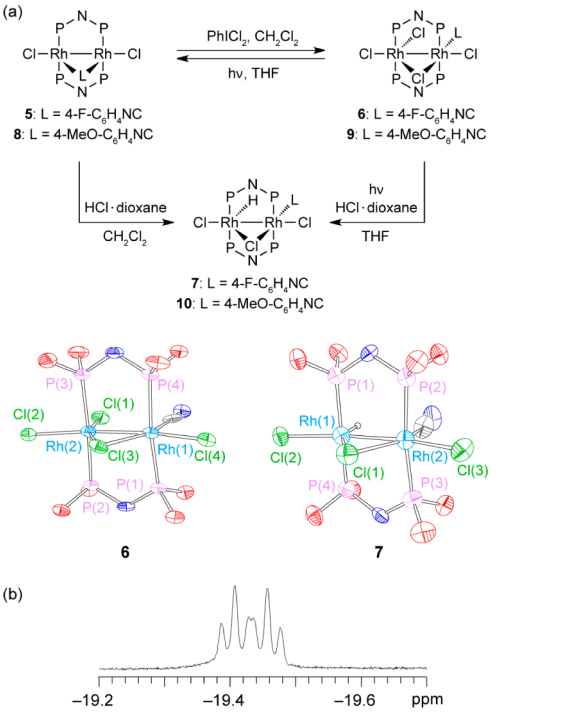

Figure 3. (a) Synthetic relationships between Rh_2L_1 chloride complexes. Thermal ellipsoid plots of **6** and **7** drawn at the 50% probability level. The $-CH_2CF_3$, aryl groups, *N*-methyl groups and hydrogen atoms are omitted for clarity. Representative bond lengths [Å]: **6**, Rh(1)−Rh(2): 2.6260(8); Rh(1)−Cl(3): 2.423(2); Rh(2)−Cl(3): 2.405(2). **7**, Rh(1)−Rh(2): 2.610(2); Rh(1)−Cl(1): 2.530(3); Rh(2)−Cl(1): 2.467(3). (b) Expansion of the upfield region of the ^{1}H NMR of Rh_2 hydride **7** showing both $^1J_{Rh-H}$ = 25.0 Hz and $^2J_{P-H}$ = 10.0 Hz.

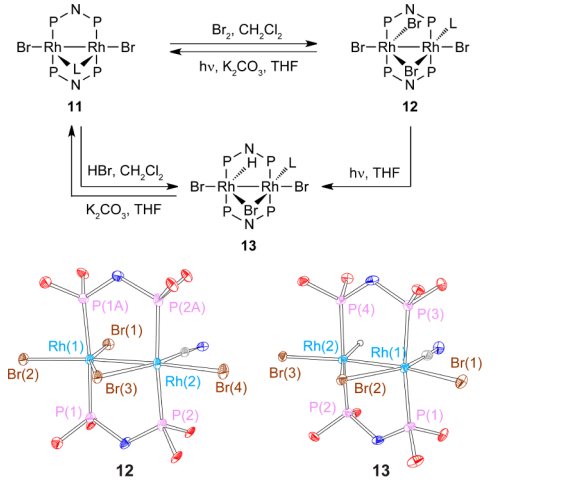

Figure 4. Synthetic relationships between Rh_2L_1 bromide complexes. Thermal ellipsoid plots of **12** and **13** drawn at the 50% probability level. The $-CH_2CF_3$, aryl groups, *N*-methyl groups and hydrogen atoms are omitted for clarity. Representative bond lengths [Å]: **12**, Rh(1)−Rh(2): 2.651(2); Rh(1)−Br(3): 2.522(2); Rh(2)−Br(3): 2.527(2). **13**, Rh(1)−Rh(2): 2.6309(6); Rh(1)−Br(2): 2.5753(7); Rh(2)−Br(2): 2.5187(7).

are similar to those observed for **7**. The ^{1}H NMR spectrum of **10** displays a resonance at −19.44 ppm that integrates for one proton (Figure S5, Supporting Information), and the IR spectrum of **10** displays a ν_{CN} = 2170 cm^{-1} (Figure S18,

dx.doi.org/10.1021/ic501136m | Inorg. Chem. 2014, 53, 9122−9128

Supporting Information), consistent with a terminally bound isocyanide ligand. In addition, single-crystal X-ray analysis reveals a close structural homology between hydrides **10** and **7**. The Rh−Cl bond trans to the hydride ligand in **10** is 2.5504(7) Å, and the Rh−Cl bond trans to the isocyanide ligand is 2.4579(7) Å.

The photochemistry of halide-bridged Rh_2L_1 complexes is not specific to Rh_2 chlorides. $Rh_2[I,I]Br_2$ complex **11**, Rh_2Br_4 **12**, and Rh_2 hydride **13** are structurally similar to their Rh_2 chloride analogues (Figure 4). Notably, the X-ray structure of Rh_2 hydride **13** was determined at 15 K using synchrotron radiation (0.41328 Å) at the Advanced Photon Source housed at Argonne National Laboratory, allowing direct location of the hydride ligand. Consistent with the structures of **7** and **10**, the Rh−Br distance to the bridging bromide is substantially longer trans to the hydride (2.6411(7) Å) than trans to the isocyanide (2.5753 (7) Å). Unlike photolysis of chloride-bridged dirhodium complexes **6** and **9** discussed above, photolysis of **12** does not lead to observation of $Rh_2[I,I]$ complex **11**, but instead leads to the evolution of the spectral features assignable to Rh_2 hydride **13** (Figure 5a). Formation of complex **13** can be envisioned as arising from initial photoreduction to Rh[I,I] complex **11** and an equivalent of Br_2. Under high photon flux conditions, Br radical formation would be expected and subsequent reaction of bromine radical with THF would afford HBr and a furanyl radical.[32] Reaction of the photoevolved HBr with $Rh_2[I,I]$ complex **11** would generate the observed Rh_2 hydride complex **13**. The Br• implied in such a scheme could arise either from homolysis of photoevolved Br_2 or directly from complex **12** via two rapid, sequential one-electron reduction steps. The dichotomous photochemical behavior of chloride-bridged Rh_2 complexes, which undergo clean photoconversion to $Rh_2[I,I]$ complexes, and the bromide-bridged Rh_2 complex **12**, which undergoes photoconversion to hydride **13**, is consistent with the increased acidity of HBr as compared to HCl (pK_a(HCl) = −0.4, pK_a(HBr) = −4.9 in 1,2-dichloroethane).[33,34] When photolysis of **12** is carried out in the presence of K_2CO_3, added to react with the photogenerated HBr, $Rh_2[I,I]$ bromide complex **11** is observed (Figure 5b).

Photocatalysis. Photocatalysis with halide-bridged complexes was investigated by irradiation of THF solutions of these complexes (1.0 mM Rh_2 catalyst) in the presence of acid (0.1 M). Evolved H_2 was quantified by both gas chromatography (GC) of the headspace gases and Toepler pump combustion analyses. Photolysis of THF solutions of **6** in the presence of HCl led to H_2 evolution. Given that halogen elimination is the efficiency-limiting step in all previous HX-splitting photocycles that we have studied, we anticipated the dirhodium tetrachloride **6** would be the photoresting state. To the contrary, UV−vis spectra of the H_2-evolution reaction catalyzed by **6** showed the disappearance of the absorption features of **6** and the evolution of the absorption spectrum of Rh_2 hydride **7** (Figure 6a). The ^{1}H NMR, IR, and UV−vis spectral features of **7** prepared by treatment of **5** with HCl are identical to those measured for **7** prepared by photolysis of **6** in the presence of HCl. Taken together, the accumulated spectral data establish that the resting state of photocatalysis is dirhodium hydride complex **7**. The change in photoresting state from the maximally chlorinated intermediate (i.e., **1**) to a Rh_2 hydride (i.e., **7**) is consistent with acceleration of halide oxidation relative to proton reduction by stabilizing the ligand-bridged structures required for the halide oxidation half-reaction (spectral overlap of complexes **6** and **7** with lamp output is pictured in Figure S29, Supporting Information). As is evident from the constant rate of H_2 evolution, and as confirmed by electronic absorption spectroscopy, no catalyst decomposition

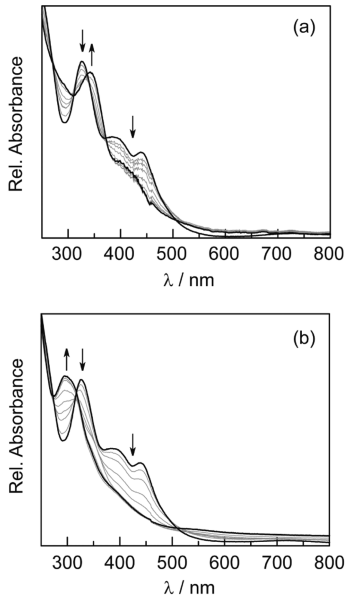

Figure 5. (a) Spectral evolution during the photolysis (λ > 295 nm, spectra collected over 100 min) of **12** in THF, which affords Rh_2 hydride **13** by reaction of photogenerated HBr with $Rh_2[I,I]$ complex **11**. (b) Spectral evolution during the photolysis (λ > 295 nm) of **12** in THF in the presence of K_2CO_3, which affords $Rh_2[I,I]$ complex **11**.

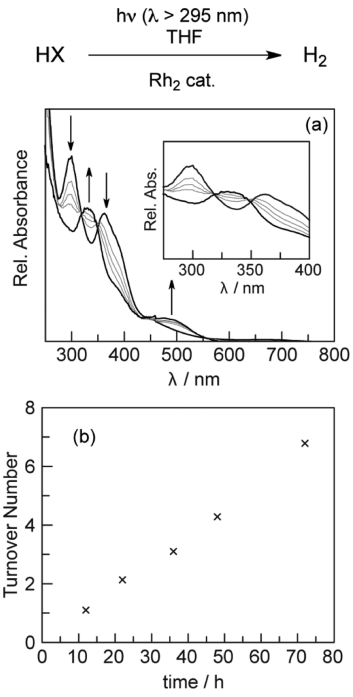

Figure 6. (a) Spectral evolution during the photolysis (λ > 295 nm, spectra collected over 75 min) of **6** in THF in the presence of HCl. The spectral features of **6** disappear and the spectral features of Rh_2 hydride **7** evolve with time. Inset: Well-anchored isosbestic points are observed, consistent conversion of **6** to **7** without a steady-state intermediate. (b) Time-dependent H_2-evolution TON (with respect to loading of catalyst **7**) from HCl, catalyzed by chloride-bridged Rh_2 complex **7**; 0.1 M HCl, 1.0 mM Rh_2 cat., λ > 295 nm.

dx.doi.org/10.1021/ic501136m | Inorg. Chem. 2014, 53, 9122−9128

is detected after 72 h of photolysis (Figure 6a). A catalyst turnover number of 6.8 is attained at 72 h.

Hydrogen evolution catalysis is also observed when chloride-bridged complex **9** is photolyzed in the presence of HCl. Similar to observations with **6** as a precatalyst, photolysis of **9** in the presence of HCl leads to the disappearance of **9** and the evolution of Rh_2 hydride **10** (Figure S26). Hydride **10** is the catalyst photoresting state during subsequent H_2 evolution. Similarly, Rh_2 hydride **13** is the photoresting state during H_2 evolution from HBr when either **11** or **12** is employed as the photocatalyst (Figure S28).

With a series of Rh_2L_1 complexes in hand, the contention that stabilization of halide-bridged geometries can provide more active HX-splitting photocatalysts could be evaluated. We examined this possibility by measuring the rate of H_2 evolution with Rh_2[II,II] complex **1** as well as chloride-bridged complexes **7** and **10** in the presence of HCl. Tetrachloride complex **1** was compared with hydridohalide complexes **7**, **10**, and **13** because each of these species represents the catalyst photoresting state during H_2-evolving photocatalysis. Consistent with Rh_2 hydrides **7**, **10**, and **13** as the catalyst resting states, the H_2-evolution profile does not change if **6**, **9**, or **12** is used as a precatalyst in lieu of complexes **7**, **10**, and **13**, respectively. To compare the H_2-evolution efficiencies of the catalysts, the amount of H_2 evolved in 24 h was measured using broadband irradiation ($\lambda > 295$ nm). The concentration of catalyst in these experiments (1.0 mM) was such that all of the incident light from the Hg arc lamp was absorbed (abs. ≥ 1.5 for $300 < \lambda < 500$ nm). Single-wavelength studies were not pursued because the overall H_2-evolution efficiency is low, which prevented reliable quantification when single wavelengths were used. We find that Rh_2L_1 complex **7** is 2.3 times more efficient in H_2 evolution than Rh_2L_2 complex **1**; and Rh_2L_1 complex **10** is 4.2 times more efficient in H_2 evolution than is complex **1**. H_2 evolution catalyzed by Br-bridged complex **12** was also found to be 3.5 times faster than H_2 evolution from HCl catalyzed by **1**.

CONCLUSIONS

Ligand photodissociation can generate reactive, unsaturated transition-metal fragments poised to participate in challenging bond making and breaking reactions.[20] Binuclear reductive elimination reactions have been proposed to proceed through ligand-bridged intermediates, which are generated from unsaturated transition-metal fragments. On the basis of the hypothesis that reactive ligand-bridged intermediates are critical to halogen photoelimination reactions from binuclear Rh complexes, we have synthesized a family of halide-bridged binuclear Rh complexes. The hypothesis that more efficient H_2-evolution catalysis could be achieved by removing the need for ligand photodissociation prior to halogen elimination reactions was interrogated by evaluating photoevolution of H_2 with the newly synthesized monoisocyanide complexes. With these catalysts, H_2 evolution, not halogen elimination, is the turnover-limiting step of photocatalysis. This observation stands in contrast to all previous binuclear HX-splitting photocatalysts, which have exhibited turnover-limiting halide oxidation. The observation of Rh_2 hydride catalyst resting states speaks to the facility of halogen elimination in these new systems. Comparison of the H_2-evolution efficacy of halide-bridged catalysts with coordinatively saturated complexes further reveals the halide-bridged structures to be 2−4 times more efficient. The increased efficiency for halide-bridged intermediates to eliminate halogen, as evidenced by the change in turnover-limiting step, and H_2 provides a new avenue to develop more efficient HX-splitting photocatalysts.

ASSOCIATED CONTENT

Supporting Information

Detailed experimental procedures and spectroscopic data for all new compounds. This material is available free of charge via the Internet at http://pubs.acs.org.

AUTHOR INFORMATION

Corresponding Author

*E-mail: dnocera@fas.harvard.edu (D.G.N.).

Notes

The authors declare no competing financial interest.

ACKNOWLEDGMENTS

We acknowledge funding from NSF Grant CHE-1332783 and a Ruth L. Kirchenstein National Research Service award (F32GM103211) for D.C.P and Dr. Yu-Sheng Chen for assistance with X-ray crystallography at ChemMatCARS, APS. ChemMatCARS Sector 15 is principally supported by the NSF/DOE under grant number NSF/CHE-1346572. Use of APS was supported by the U.S. DOE, Office of Science, Office of Basic Energy Sciences, under Contract No. DE-AC02-06CH11357.

REFERENCES

(1) Cook, T. R.; Dogutan, D. K.; Reece, S. Y.; Surendranath, Y.; Teets, T. S.; Nocera, D. G. *Chem. Rev.* **2010**, *110*, 6474−6502.
(2) Rüttinger, W.; Dismukes, G. C. *Chem. Rev.* **1997**, *97*, 1−24.
(3) Yagi, M.; Kaneko, M. *Chem. Rev.* **2001**, *101*, 21−35.
(4) McEvoy, J. P.; Brudvig, G. W. *Chem. Rev.* **2006**, *106*, 4455−4483.
(5) Esswein, A. J.; Nocera, D. G. *Chem. Rev.* **2007**, *107*, 4022−4047.
(6) Lin, T.-P.; Gabbaï, F. P. *J. Am. Chem. Soc.* **2012**, *134*, 12230−12238.
(7) Karikachery, A. R.; Lee, H. B.; Masjedi, M.; Ross, A.; Moody, M. A.; Cai, X.; Chui, M.; Hoff, C. D.; Sharp, P. R. *Inorg. Chem.* **2013**, *52*, 4113−4119.
(8) Carrera, E. I.; McCormick, T. M.; Kapp, M. J.; Lough, A. J.; Seferos, D. S. *Inorg. Chem.* **2013**, *52*, 13779−13790.
(9) Lee, C. H.; Lutterman, D. A.; Nocera, D. G. *Dalton Trans.* **2013**, *42*, 2355−2357.
(10) Nocera, D. G. *Inorg. Chem.* **2009**, *48*, 10001−10017.
(11) Cotton, F. A.; Nocera, D. G. *Acc. Chem. Res.* **2000**, *33*, 483−490.
(12) Heyduk, A. F.; Nocera, D. G. *Science* **2001**, *293*, 1639−1641.
(13) Esswein, A. J.; Veige, A. S.; Nocera, D. G. *J. Am. Chem. Soc.* **2005**, *127*, 16641−16651.
(14) Elgrishi, N.; Teets, T. S.; Chambers, M. B.; Nocera, D. G. *Chem. Commun.* **2012**, *48*, 9474−9476.
(15) Gray, T. G.; Veige, A. S.; Nocera, D. G. *J. Am. Chem. Soc.* **2004**, *126*, 9760−9768.
(16) Powers, D. C.; Chambers, M. B.; Teets, T. S.; Elgrishi, N.; Anderson, B. L.; Nocera, D. G. *Chem. Sci.* **2013**, *4*, 2880−2885.
(17) Norton, J. R. *Acc. Chem. Res.* **1979**, *12*, 139−145.
(18) Martin, B. D.; Warner, K. E.; Norton, J. R. *J. Am. Chem. Soc.* **1986**, *108*, 33−39.
(19) Kristjánsdóttir, S. S.; Norton, J. R. In *Transition Metal Hydrides*; Dedieu, A., Ed.; VCH: New York, 1992; Chapter 9, p 309.
(20) Arndtsen, B. A.; Bergman, R. G.; Mobley, T. A.; Peterson, T. H. *Acc. Chem. Res.* **1995**, *28*, 154−162.
(21) Pangborn, A. B.; Giardello, M. A.; Grubbs, R. H.; Rosen, R. K.; Timmers, F. J. *Organometallics* **1996**, *15*, 1518−1520.
(22) Ahmed, W.; Gerrard, W.; Maladkar, V. K. *J. Appl. Chem.* **1970**, *20*, 109−116.
(23) Teets, T. S.; Cook, T. R.; Nocera, D. G. *Inorg. Synth.* **2010**, *35*, 164−168.

(24) Giordano, G.; Crabtree, R. H. *Inorg. Synth.* **1990**, *28*, 88−90.
(25) Wallace, T. J.; Gritter, R. J. *J. Org. Chem.* **1962**, *27*, 3067−3071.
(26) Mignani, S.; Beaujean, M.; Janousek, Z.; Merenyi, R.; Viehe, H. G. *Tetrahedron* **1981**, *37*, 111−115.
(27) Yamamoto, Y. *Coord. Chem. Rev.* **1980**, *32*, 193−233.
(28) Robertson, M. J.; Angelici, R. J. *Langmuir* **1994**, *10*, 1488−1492.
(29) Malatesta, L.; Bonati, F. *Isocyanide Complexes of Metals*; John Wiley: New York, 1969; pp 25−29.
(30) Spessard, G. O.; Miessler, G. L. *Organometallic Chemistry*; Prentice-Hall: Upper Saddle River, NJ, 1997; pp 140−145.
(31) Teets, T. S.; Nocera, D. G. *J. Am. Chem. Soc.* **2011**, *133*, 17796−17806.
(32) Lo, J. M. H.; Marriott, R. A.; Giri, B. R.; Roscoe, J. M.; Klobukowski, M. *Can. J. Chem.* **2010**, *88*, 1136−1145.
(33) Raamat, E.; Kaupmees, K.; Ovsjannikov, G.; Trummal, A.; Kütt, A.; Saame, J.; Koppel, I.; Kaljurand, I.; Lipping, L.; Rodima, T.; Pihl, V.; Koppel, I. A.; Leito, I. *J. Phys. Org. Chem.* **2013**, *26*, 162−170.
(34) Kütt, J.; Rodima, T.; Saame, J.; Raamat, E.; Mäemets, V.; Kaljurand, I.; Koppel, I. A.; Garlyauskayte, R. Y.; Yagupolskii, Y. L.; Yagupolskii, L. M.; Bernhardt, E.; Willner, H.; Leito, I. *J. Org. Chem.* **2011**, *76*, 391−395.